Geochimica et Cosmochimica Acta 397 (2025) 1–12

Contents lists available at ScienceDirect

Geochimica et Cosmochimica Acta

journal homepage: www.elsevier.com/locate/gca

Basin-scale production of hyperacidic brines is critical for the formation of high-grade and large-tonnage uranium deposits in sedimentary basins

Yumeng Wang [a,b], Guoxiang Chi [a,*], Sean A. Bosman [c]

[a] Department of Earth Sciences, University of Regina, Regina, Saskatchewan S4S 0A2, Canada
[b] IFN-2, Forschungszentrum Jülich GmbH, Jülich, North Rhine-Westphalia 52428, Germany
[c] Saskatchewan Geological Survey, Regina, Saskatchewan S4P 2C7, Canada

ARTICLE INFO

Associate editor: Benjamin Tutolo

Keywords:
Hyperacidic brines
pH
Sedimentary basins
Diagenesis
Fluid-rock interaction
Kaolinite-illite
Uranium deposits
Athabasca Basin

ABSTRACT

Unconformity-related uranium deposits (URU deposits) in the Proterozoic Athabasca Basin (Canada) represent the largest and richest (with average grades ranging from 0.127 to 19.5 wt% U) U deposits in the world. Fluid inclusion studies and experimental data suggest that the ore-forming fluids of URU deposits are hyperacidic (pH < 3.5), oxidizing basinal brines carrying high concentrations of U (0.2 to 3700 ppm), which are several orders of magnitude higher than ordinary basinal and basement formation waters. While the oxidizing conditions of these fluids are well established, the mechanism responsible for the basin-scale generation of hyperacidic brines remains unknown. This paper aims to address this problem and to explain why the Athabasca Basin is exceptionally endowed with high-grade and large-tonnage uranium deposits. Based on petrographic and infrared hyperspectral logging data indicating basin-wide coexistence of kaolinite and illite in quartz-dominated sandstones, and fluid inclusion data showing high potassium (K) concentrations in diagenetic and ore-forming fluids within the Athabasca Basin, it is proposed that the production of hyperacidic brines resulted from a pervasive diagenetic reaction between K-rich brines and kaolinite: 3kaolinite $[Al_2Si_2O_5(OH)_4]$ + 2 K^+ ↔ 2illite $[KAl_3Si_3O_{10}(OH)_2]$ + $3H_2O$ + $2H^+$. Geochemical modeling of fluid-rock reactions demonstrates that the basin-scale production of hyperacidic brines is achievable when a combination of three specific conditions is satisfied: 1) the presence of a thick package of compositionally mature sandstones, characterized by quartz-dominated framework grains with minimal (<1%) feldspar and the interstitial space filled with kaolinite; 2) the development of K-rich brines through seawater evaporation above the sandstone package; and 3) low fluid/rock ratios, which enable the reaction between kaolinite and K-rich brines to reach equilibrium and produce illite and H^+. Recognizing the basin-scale development of hyperacidic brines and the specific conditions entailed offers insights into why the Athabasca Basin is exceptionally endowed with high-grade, large-tonnage U deposits. The conditions of hyperacidic brine production revealed in this study may be used for evaluating the U mineralization potential of other sedimentary basins.

1. Introduction

Uranium (U) is a critical metal that plays an important role in the era of energy and economy transformation toward low-emission and sustainable systems (NEA-IAEA, 2023). Global U resources are dominantly hosted by, and produced from, sedimentary basins, particularly from two types of U deposits, i.e., sandstone-hosted and unconformity-related (Kyser and Cuney, 2015; IAEA, 2018). While sandstone-hosted U (SHU) deposits are widespread in Phanerozoic basins, particularly Mesozoic and Cenozoic, unconformity-related U (URU) deposits, which typically occur near the unconformity between sedimentary basins and the underlying metamorphosed basement, are primarily concentrated in a few Proterozoic basins in Canada and Australia (Kyser and Cuney, 2015; IAEA, 2018). The principal SHU deposits are characterized by relatively low grades (0.013 – 0.49 wt% U) and variable tonnages (1,135 – 276,200 t U), whereas the URU deposits feature high grades (0.127 – 19.5 wt% U) and large tonnages (15,560 – 261,000 t U) (IAEA, 2018; Fig. 1A). Among the URU deposits, those in the Athabasca Basin in Canada have particularly high grades, with the average grades being mostly > 2 wt% U (Fig. 1A). Considering a crustal U abundance of 1.8 ppm (Mason and Moore, 1982), such high average grades correspond to concentration factors of ~ 10,000 to ~ 100,000 (Chi et al., 2019), which

* Corresponding author.
E-mail address: Guoxiang.Chi@uregina.ca (G. Chi).

https://doi.org/10.1016/j.gca.2025.03.031
Received 26 November 2024; Accepted 29 March 2025
Available online 4 April 2025

are much higher than normal concentration factors of only a few hundreds to a few thousands for most metallic ores (Robb, 2020). While bonanzas are locally developed in many geological settings, the occurrence of a large number of high-grade ore deposits within a single basin is unusual, and the mechanism behind this phenomenon remains unclear. Understanding this mechanism has important implications on the ore genesis, geochemical behavior of U and further exploration for U resources in sedimentary basins.

Fluid inclusion studies of the URU deposits in the Athabasca Basin, and those in quartz overgrowths in sandstones within the basin, indicate that the ore-forming fluids were derived from basinal brines with temperatures mainly from 80 to 200℃, salinities mainly from 25 to 35 wt%, and a composition system of H_2O-NaCl-$CaCl_2$-$MgCl_2$-KCl (Pagel, 1975; Kotzer and Kyser, 1995; Derome et al., 2005; Richard et al., 2012, 2016; Chu and Chi, 2016; Chi et al., 2019; Wang et al., 2018; Martz et al., 2019; Rabiei et al., 2021, 2023; Ferguson et al., 2025). Furthermore, the Cl/Br and $\delta^{37}Cl$ analysis of fluid inclusions (Richard et al., 2011), and the $\delta^{11}B$ analysis of Mg-rich tourmaline associated with URU mineralization (Mercadier et al., 2012; Potter et al., 2022), indicate that the basinal brines originated from seawater evaporation beyond halite saturation, up to sylvite saturation (Richard et al., 2011). The ubiquitous development of hematite within the sandstones and underlying paleoregolith, with no coexisting magnetite, indicates that the basinal brines were oxidizing (above the hematite/magnetite buffer), and U was dissolved mainly as U(VI) in the form of uranyl (UO_2^{2+}) chlorine complexes (Hoeve and Quirt, 1984; Kotzer and Kyser, 1995). Thermodynamic calculations suggest that for U solubility to reach ~ 17 ppm at 200 °C with an assumed pH of 4.45, the log fO_2(g) must be above − 24, which is well above the hematite-magnetite buffer (log fO_2(g) = − 39.5 at 200 °C) (Komninou and Sverjensky, 1996). All these results support the "diagenetic-hydrothermal" model proposed by Hoeve and Sibbald (1978), in which oxidizing basinal brines circulated within oxidizing sandstones, extracted U from sandstones and/or basement rocks, and then precipitated uraninite near the basal unconformity upon interaction with reducing lithologies and/or basement-derived fluids (Jefferson et al., 2007; Kyser and Cuney, 2015). However, while this model satisfactorily explains the geological and geochemical characteristics of the URU deposits (Hoeve and Sibbald, 1978; Hoeve and Quirt, 1984; Jefferson et al., 2007; Kyser and Cuney, 2015), it does not offer a mechanism to explain why such large and rich deposits developed only in the Athabasca Basin.

An important breakthrough in addressing the above problem was the discovery of exceptionally high U concentrations (up to 3700 ppm) in fluid inclusions associated with URU deposits in the Athabasca Basin (Richard et al., 2012, 2016; Martz et al., 2019; Rabiei et al., 2023; Ferguson et al., 2025). These concentrations are several orders of magnitude higher than those in most natural fluids, including basin and basement formation waters (Fig. 1B). The high concentrations of U in the ore-forming fluids have been invoked as a necessary requirement for the formation of giant U deposits in relatively short periods of time of about 0.1–1 Myr (Richard et al., 2012). Another significant finding is the widespread development of U-rich diagenetic fluids similar to the ore-forming fluids, as recorded by fluid inclusions in quartz overgrowths in sandstones of the Athabasca Basin, suggesting that U for URU mineralization was mainly derived from the basin rather than the basement (Chi et al., 2019). Several lines of evidence support this interpretation: 1) URU deposits occur in different locations of the basin, underlain by basement rocks belonging to different cratons with diverse lithologies and U contents (Rabiei et al., 2023); 2) geochemical modeling shows oxidizing and hyperacidic basinal brines quickly lose their capability to dissolve and transport high concentrations of U due to fluid-rock interactions when infiltrating basement rocks (Wang et al., 2024); and 3) reactive transport modeling demonstrates that the abundance of U-rich diagenetic fluids in the basin is essential for URU mineralization (Wang and Chi, 2023). Given these recent advancements, the question of why the Athabasca Basin is so favorable for the

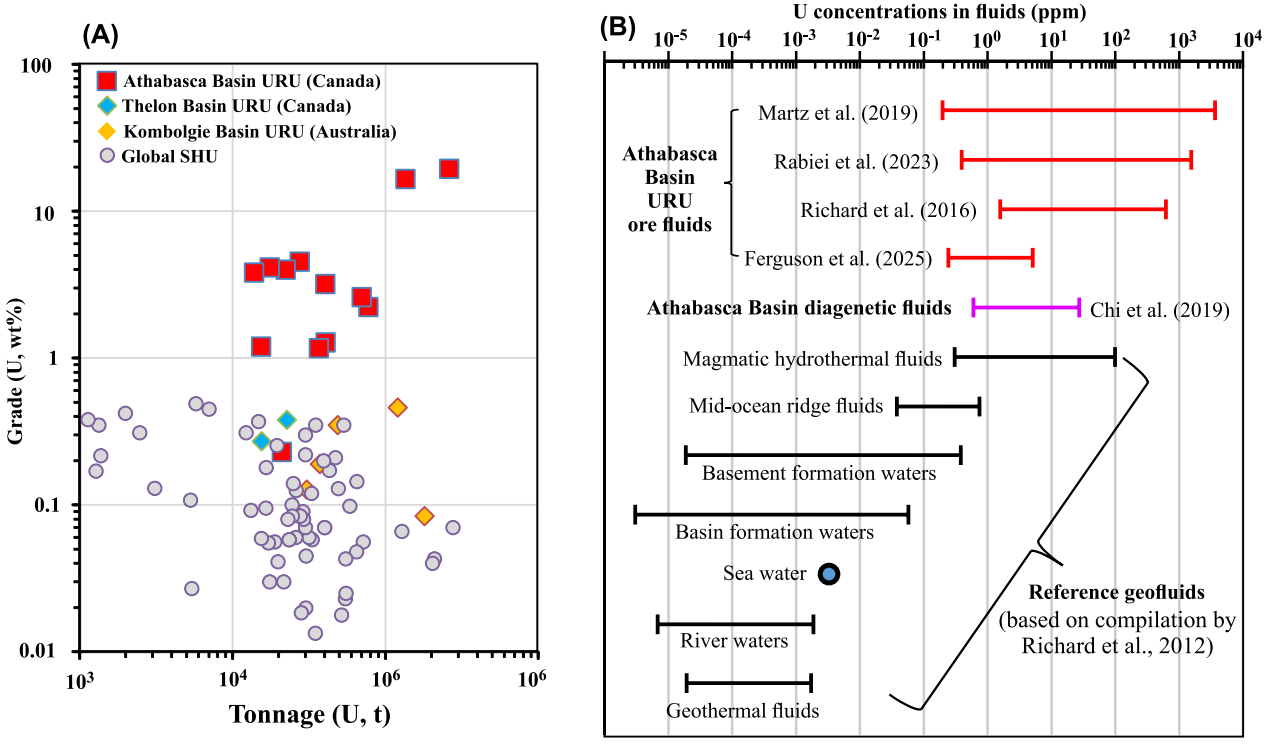

Fig. 1. (A) Metal tonnage – grade diagram of unconformity-related uranium (URU) deposits, including those in the Athabasca Basin (Canada), Thelon Basin (Canada), and Kombolgie Basin (Australia), and sandstone-hosted uranium (SHU) deposits (global); data from IAEA (2018); (B) Concentrations of uranium in fluid inclusions from URU deposits (Richard et al., 2016; Martz et al., 2019; Rabiei et al., 2023; Ferguson et al., 2025) and fluid inclusions in quartz overgrowths in sandstone (Chi et al., 2019) in the Athabasca Basin, in comparison with concentrations of uranium in various natural fluids (Richard et al., 2012).

development of URU deposits then becomes why U-rich brines were favorably developed in this basin.

Although U(VI) is much more soluble than U(IV) and can form complexes with various ligands, including Cl^-, OH^-, F^-, SO_4^{2-}, PO_4^{3-}, and CO_3^{2-} (Romberger, 1984), uranyl chlorine complexes, particularly UO_2Cl^+ and UO_2Cl_2(aq), are likely the dominant dissolved U species in the ore-forming brines of the Athabasca Basin. This is supported by the high Cl^- concentrations in basinal brines and the high formation constants of uranyl chlorine complexes under URU mineralization conditions (Richard et al., 2012; Dargent et al., 2013, 2015; Migdisov et al., 2018). The presence of fluorapatite and aluminum-phosphate-sulfate (APS) minerals in the sandstone suggests that F^-, SO_4^{2-}, and PO_4^{3-} were present in the basinal brines, but the low solubility of these minerals in the presence of Ca^{2+} in the basinal brines makes the concentrations of these anions subordinate compared to Cl^- in U complexation (Gaboreau et al., 2007). Additionally, the scarcity of carbonate minerals and the instability of uranyl carbonate complexes above 100 °C suggest that CO_3^{2-} played a negligible role in U(VI) mobility (Kalintsev et al., 2021). Recent experimental studies on U(VI) solubility in oxidizing brines (Richard et al., 2012; Dargent et al., 2013, 2015; Migdisov et al., 2018) and thermodynamic modeling incorporating updated experimental data (Xing et al., 2018; Deng et al., 2023; Wang et al., 2024) consistently suggest that if U(VI) was primarily dissolved as uranyl chlorine complexes, the ore-forming fluids must have a pH < 3.5 to account for the anomalously high U solubilities observed in fluid inclusions. However, the mechanisms responsible for the generation of such hyperacidic brines remain enigmatic. Therefore, the question why the Athabasca Basin hosts exceptionally high-grade, large-tonnage U deposits further becomes why this basin is exceptionally favorable for the large-scale generation of hyperacidic brines.

This study presents a novel model in which voluminous hyperacidic brines with pH values < 3.5 are produced through the reaction between K-rich brines and thick successions of quartz-dominated, kaolinite-bearing, feldspar-poor sandstones. The model is supported by petrographic observations and infrared hyperspectral logging data indicating basin-wide coexistence of kaolinite and illite in the sandstones, and fluid inclusion data indicating high concentrations of K in the basinal brines of the Athabasca Basin. Geochemical modeling of fluid-rock reactions was conducted to examine whether, and under what conditions, hyperacidic brines can form through diagenetic processes in sandstones. The special geological and geochemical conditions required to produce such hyperacidic brines, which facilitate the extraction of U from fertile source rocks, can explain why the Athabasca Basin is exceptionally favorable for the formation of high-grade, large-tonnage U deposits. The results of this study also provide insights into the identification of geological conditions required for the production and preservation of hyperacidic brines in other sedimentary basins, which have important implications for the formation of high-grade U deposits as well as other types of sediment-hosted mineral deposits.

2. Geological background

The Athabasca Basin is a Paleo- to Mesoproterozoic intracratonic basin developed on the Canadian Shield (Fig. 2A; Jefferson et al., 2007). It unconformably overlies the Archean to Paleoproterozoic metamorphic basement of the Rae craton in the west and the Hearne craton in the east, flanked by the Taltson magmatic zone and Thelon orogenic belt to the west, and the Trans-Hudson orogen to the east (Card et al., 2021). The preserved sedimentary rocks are generally flat-lying, indicating that the basin has not experienced significant tectonic deformation, except for considerable exhumation (Jefferson et al., 2007; Ramaekers et al., 2007). This has resulted in a remnant sedimentary succession with a maximum thickness of ~ 1,500 m, dominantly composed of variably hematitic, medium- to coarse-grained, fluviatile quartzose sandstones, with minor components of fluviatile conglomerates, lacustrine/marine mudstones and marine carbonates (Ramaekers et al., 2007).

The sedimentary succession in the Athabasca Basin was initially assigned to the Athabasca Group (Ramaekers et al., 2007), which was later designated as part of the Athabasca Supergroup that includes the older Martin Group in the Martin Basin (Bosman and Ramaekers, 2015). The rocks in the Athabasca Basin are divided into four groups in the Athabasca Supergroup, i.e., from bottom to top, the Fair Point, Manitou Falls, Lazenby Lake, Wolverine Point, and MacFarlane groups (Bosman and Ramaekers, 2015). The sedimentary succession in the Athabasca Basin can be divided into five lithostratigraphic packages, i.e., from bottom to top, a lower fluviatile sandstone package including the Fair Point, Manitou Falls and Lazenby Lake groups, a middle lacustrine mud-bearing package comprising the Wolverine Point Group, an upper fluviatile sandstone package consisting of the Locker Lake and Otherside formations, an upper marine shale-dominated package comprising the

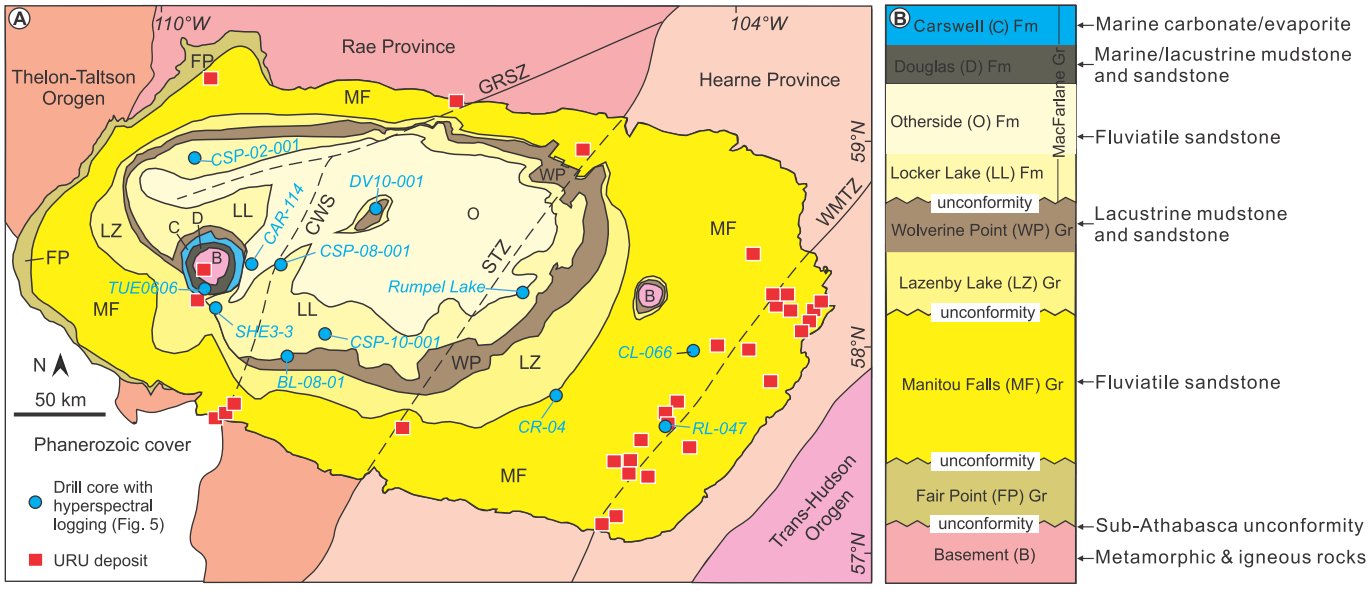

Fig. 2. (A) Generalized geological map of the Athabasca Basin stratigraphic units (Bosman and Ramaekers, 2015) and locations of significant URU deposits and drillholes from which hyperspectral logging data were collected (Fig. 5). CWS – Clearwater structure; STZ – Snowbird tectonic zone; WMTZ – Wollaston-Mudjatik transition zone; GRSZ – Grease River shear zone. (B) Generalized lithostratigraphic column. Gr – Group, Fm – Formation.

Douglas Formation, and a marine dolomitic package comprising the Carswell Formation, all as part of the MacFarlane Group (Fig. 2B). Deposition of the Fair Point Group may have started as early as 1810 Ma, based on the youngest detrital zircon age, although the precise age is currently unknown (Rainbird et al., 2007). A U-Pb age of ca. 1644 Ma was reported for igneous zircon in a tuffaceous unit of the Wolverine Point Group (Rainbird et al., 2007), and a Re-Os isochron age of ca. 1541 Ma was obtained for carbonaceous shales in the Douglas Formation (Creaser and Stasiuk, 2007). Isopach maps of the various stratigraphic units and structural contours of the basal unconformity surface suggest that the sedimentation distribution was influenced by basement faults (Ramaekers et al., 2007, 2017; Maxeiner et al., 2021).

The fluviatile sandstones are characterized as continental red beds, with hematite either as pore-filling material or as fine-grained coatings on quartz grains. They account for > 90 % of the total volume of the preserved sedimentary rocks in the Athabasca Basin and are dominantly composed of detrital quartz grains (~99 vol%), with near-complete lack of preserved feldspar grains across the basin (Ramaekers et al., 2007; Bosman and Ramaekers, 2015; Chu et al., 2015). The interstitial materials are mainly composed of clay minerals dominated by kaolinite/dickite and illite, with minor amounts of chlorite, tourmaline and aluminum-phosphate-sulfate (APS) minerals (Hoeve and Quirt, 1984; Kister et al., 2005; Chu et al., 2015; Percival et al., 2018).

The URU deposits in the Athabasca Basin are generally located near the basal unconformity of the basin and associated with reactivated basement faults. Most of the URU deposits are distributed along regional fault zones, including the Wollaston-Mudjatik transitional zone (WMTZ), Snowbird tectonic zone (STZ) and Clearwater structure (CWS) (Fig. 2A). The oldest URU mineralization may have occurred at ca. 1590 Ma (Alexandre et al., 2009), but the most significant URU mineralization, represented by the McArthur River deposit (the largest URU deposit in the Athabasca Basin), likely occurred between 1540 and 1570 Ma, as constrained by a uraninite U-Pb isotopic age of ca. 1540 Ma (Alexandre et al., 2009) and an anatase U-Pb isotopic age of ca. 1569 Ma (Adlakha and Hattori, 2021) from that deposit. These ages are also consistent with a xenotime U-Pb age of ca. 1547 Ma from the Maw Zone rare earth element deposit, which shows similar alteration assemblages as the McArthur River deposit (Rabiei et al., 2017). The inferred age (1540–1570 Ma) for the major URU mineralization is consistent with the generation of basinal brines associated with the marine environments that formed the Carswell Formation, which immediately overlies the ca. 1541 Ma Douglas Formation (Creaser and Stasiuk, 2007), supporting a genetic link between the development of basinal brines and URU mineralization (Chi et al., 2018).

3. Data and Methods

This study uses data compiled from the literature to establish a hypothesis for the development of hyperacidic brines in the Athabasca Basin and then uses geochemical reaction path modeling to test this hypothesis. Fluid composition data were from laser ablation inductively coupled plasma mass spectrometry (LA-ICP-MS) analyses of fluid inclusions reported by Richard et al. (2012, 2016), Chi et al. (2019), Martz et al. (2019), Rabiei et al. (2023), and Ferguson et al. (2025). The analytical methods and original data can be found in these studies, and the data used in this study are compiled in the supplementary material. The data for the basin-wide distribution of the proportions of different clay minerals (and some non-clay minerals) were from core logging using hand-held SWIR (short-wave infrared: 1200–2500 nm) and VNIR (visible near-infrared: 380–1200 nm) spectrometers as reported by Bosman and Percival (2014) and Percival et al. (2018). These methods have been widely used to determine the mineralogy of sedimentary rocks in both outcrops and drill cores, as described by Bowen et al. (2007) and Okyay and Khan (2016). The locations of the drill cores with logging data in this study are shown in Fig. 2A. The original data and procedures for logging data processing are provided in the supplementary material. Selected polished thin sections of sandstones that were previously studied for petrography (Scott et al., 2012; Chu et al., 2015) were re-examined with scanning electron microscopy – energy dispersive X-ray spectroscopy (SEM-EDS) for textural relationships between clay minerals. The SEM-EDS analysis was carried out at the University of Regina (Saskatchewan, Canada) using a TESCAN VEGA3 SEM equipped with an Edax EDS system.

Reaction path modeling was performed using the Geochemist's Workbench (GWB) software (Bethke, 2022). The goal was to verify whether hyperacidic brines with pH < 3.5 could be produced through fluid-rock interaction and identify the conditions under which such brines could form. This was done by testing various scenarios involving different fluid compositions, sandstone compositions, fluid/rock ratios and temperatures. The thermodynamic data for aqueous species, minerals, and the B-dot model for calculating activity coefficients of charged aqueous species were all adopted from the standard Lawrence Livermore National Laboratory (LLNL) thermodynamic database as implemented in GWB (Bethke, 2022). The modeled fluid-rock system was assumed to be in thermodynamic equilibrium, justified by the protracted contact and reaction time between diagenetic fluids and sandstones, as well as the elevated burial temperatures (80–200℃) in the Athabasca Basin.

The conceptual model was designed by incrementally adding sandstone with a specified mineral composition to a total of 1 kg of brine with a specified initial fluid composition. As sandstone was progressively added, the fluid/rock mass ratio decreased from 10^5 (after adding 10^{-5} kg of sandstone) to 1 (after adding 1 kg of sandstone). Nine scenarios were tested (Fig. 3), with Scenario 1 (Fig. 3A) serving as the base model, in which the sandstone is composed of 99 vol% quartz and 1 vol% kaolinite, with no K-feldspar or albite. The initial fluid was assumed to be a brine with a pH of 6 at 120℃, a temperature consistent with typical burial diagenetic temperatures recorded in fluid inclusions from the Athabasca Basin (Pagel, 1975; Chu and Chi, 2016). The pH of 6 is considered circumneutral at 120℃ and is reasonable for basinal brines derived from seawater evaporation. Based on compiled fluid inclusion data, the initial fluid was assigned concentrations of 213,000 ppm Cl, 132,117 ppm Na, and 10,000 ppm K. The Si concentration was set at 14.67 ppm, based on equilibrium with detrital quartz. The Al concentration was set at 2.7×10^{-5} ppm (10^{-9} M), consistent with typical Al concentrations in evaporated seawater and its low solubility under near-neutral conditions.

Scenarios 2 to 9 were designed by modifying one parameter at a time from the base model of Scenario 1 (Fig. 3B) to evaluate the effects of initial K concentration in the brine, kaolinite and feldspar content in the sandstone, and temperature on the modeling results. Scenarios 2 and 3 examine the effects of lower (1,000 ppm) and higher (25,000 ppm) K concentrations in the brine. The 1,000 ppm K concentration represents evaporated seawater between gypsum and halite saturation, while 25,000 ppm K corresponds to a point near sylvite saturation. Scenarios 4 and 5 investigate the impact of varying kaolinite content in the sandstone by testing a lower (0.1 vol%) and a higher (10 vol%) value. Scenarios 6 and 7 evaluate the influence of 1 vol% and 5 vol% K-feldspar in the sandstone. Although K-feldspar is essentially absent in the Athabasca Basin sandstones, minor amounts (1–5 vol%) of K-feldspar have been reported in the Thelon Basin (Jefferson et al., 2007; Hiatt et al., 2010), which hosts fewer, smaller, and lower-grade URU deposits. Therefore, Scenarios 6 and 7 were designed to evaluate whether K-feldspar content can affect the ore-forming potential of the fluid. Scenarios 8 and 9 examine the impact of higher (200℃) and lower (80℃) temperatures. The 200℃ represents the peak diagenetic and mineralization conditions in the Athabasca Basin, as estimated from fluid inclusion and clay geothermometric studies (Pagel, 1975; Kotzer and Kyser, 1995; Chu and Chi, 2016), while 80℃ may correspond to a shallow burial stage before the basin reached its maximum burial depth (Chi et al., 2018).

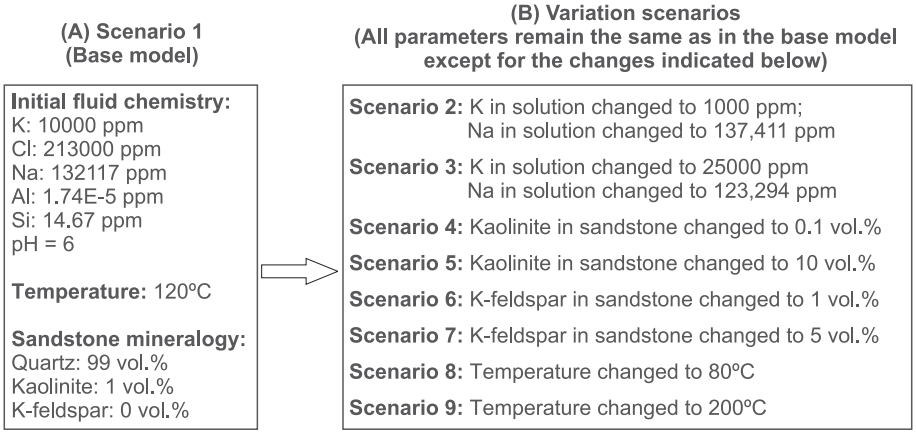

Fig. 3. Initial sandstone and fluid compositions used in different scenarios of geochemical path modeling of fluid-rock interaction. Scenario 1 (A) is the base model, and each of Scenarios 2 to 9 (B) is deviated from the base model by changing one parameter.

4. Results

4.1. Concentrations of K and Cl in basinal brines

The concentrations of K and Cl in basinal brines were compiled from fluid inclusion analyses reported in the literature (Richard et al., 2016; Chi et al., 2019; Martz et al., 2019; Rabiei et al., 2023; Ferguson et al., 2025) and summarized in the supplementary material. The concentrations of Cl range from 68,848 to 290,885 ppm, with an average of 204,827 ppm. The concentrations of K range from 403 to 86,924 ppm, with an average of 10,812 ppm. In the K-Cl diagram (Fig. 4), the fluid inclusion data mostly fall within the range extending from immediately before halite saturation to after sylvite saturation along the seawater evaporation path (Fontes and Matray, 1993). The concentrations of K are mainly between the values at halite saturation (~8,500 ppm) and sylvite saturation (~26,000 ppm) (Fig. 4).

4.2. Basin-scale distribution pattern of clay minerals in sandstones

The basin-scale distribution of clay minerals in the sandstones of the Athabasca Basin is established based on infrared hyperspectral logging data of drill cores across the basin (Fig. 2A; Bosman and Percival, 2014; Percival et al., 2018). The identified mineral groups include kaolin (kaolinite, dickite, nacrite), white mica (illite, muscovite, paragonite), chlorite (Fe-chlorite, Fe-Mg-chlorite, Mg-chlorite), epidote (epidote, zoisite), smectite (montmorillonite, nontronite), tourmaline (Fe-Tourmaline, Mg-Tourmaline), amphibolite (hornblende), diaspore, carbonate (calcite, ankerite, dolomite, siderite), and sulfate (gypsum, alunite). The original data are provided in the supplementary material. These minerals are combined into three groups: “kaolinite” group (well-crystalline kaolinite, poor-crystalline kaolinite, dickite, nacrite), “illite” group (muscovite, muscovitic illite, phengitic illite, paragonitic illite), and “others”, with their relative proportions detailed in the supplementary material. By plotting these data as a function of depth across 12

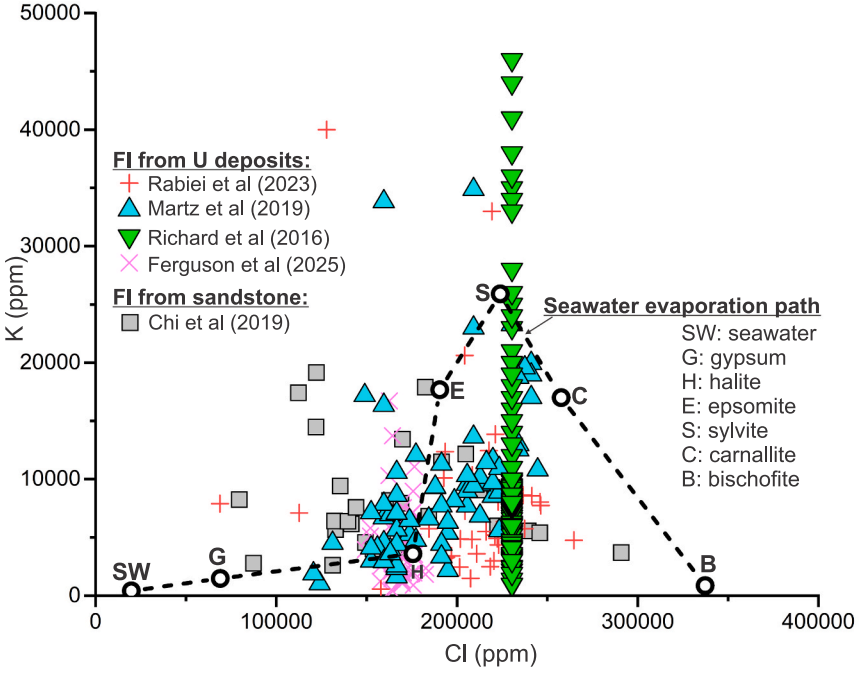

Fig. 4. Diagram showing K-Cl concentrations in fluid inclusions from URU deposits (Richard et al., 2016; Martz et al., 2019; Rabiei et al., 2023; Ferguson et al., 2025) and sandstone quartz overgrowths in the Athabasca Basin (Chi et al., 2019). Note a chlorinity of 6.5 molal was assumed for all fluid inclusions by Richard et al. (2016). The seawater evaporation path is from Fontes and Matray (1993).

drill cores, a basin-scale pattern of the prominent coexistence of "kaolinite" and "illite" and their dominance as interstitial minerals between detrital quartz grains are revealed (Fig. 5). "Kaolinite" and "illite" consistently occur within the same depth intervals across all drill cores, although their relative proportions vary between cores (Fig. 5). The "others" group appears sporadically throughout the drill cores, generally in low proportions, with a slight tendency to be more concentrated at greater depths near or within the basement (Fig. 5).

4.3. Petrographic observations on the relationship between kaolinite/dickite and illite

Petrographic examination of thin sections of sandstone samples and SEM-EDS analyses consistently show that kaolinite/dickite and illite are the dominant clay minerals in the sandstones of the Athabasca Basin. The coexistence of well-crystallized kaolinite or dickite with illite in the interstitial space between quartz grains was observed in most of the samples examined (Fig. 6A, B). Authigenic, needle-shaped illite typically interweaves with kaolinite/dickite or fills the open space between kaolinite/dickite crystals (Fig. 6C, D). Locally, illite crosscuts kaolinite/dickite or wraps the latter as "reaction rims" (Fig. 6D). These textural relationships indicate that kaolinite/dickite was present before illite, and illite likely developed from the reaction of kaolinite/dickite with permeating K-rich fluid. Furthermore, the ubiquitous coexistence of these two minerals suggests that the reaction reached equilibrium in most parts of the basin.

4.4. Geochemical reaction path modeling results

Geochemical reaction path modeling was conducted for nine scenarios involving different initial fluid and sandstone compositions and temperatures (Fig. 3). In each scenario, up to 1 kg of sandstone was incrementally added to 1 kg of brine, corresponding to decreasing the fluid/rock mass ratio gradually from 10^5 to 1. The modeling results, illustrating changes in pH and mineral proportions as a function of reacted sandstone mass or fluid/rock mass ratio, are shown in Fig. 7.

The results for Scenario 1 (base model) indicate that a pH of 3.4 can be achieved at a fluid/rock mass ratio of < 40, together with the development of both kaolinite and illite (Fig. 7A). In Scenario 2, with the initial K concentration in the brine being reduced from 10,000 ppm in the base model to 1,000 ppm, the minimum pH that can be achieved is 4.4 (Fig. 7B). Conversely, if the initial K concentration increases to 25,000 ppm, the minimum pH drops to 3.0, as shown in Scenario 3 (Fig. 7C). Changing the initial content of kaolinite in the sandstone to a lower value (0.1 vol%, Scenario 4, Fig. 7D) or a higher value (10 vol%, Scenario 5, Fig. 7E) have no effect on the minimum pH value (3.4) during the brine-sandstone interaction. However, the fluid/rock mass ratio at which this pH is achieved varies depending on the initial kaolinite content. A comparison of Fig. 7D and Fig. 7E indicates that higher kaolinite content in the sandstone promotes the development of low-pH brines at higher fluid/rock mass ratios. Adding a minor amount of K-feldspar (1 vol%, Scenario 6) to the initial sandstone does not affect the minimum pH either, as the K-feldspar is completely replaced by the kaolinite + illite assemblage at low fluid/rock mass ratios (Fig. 7F). However, if the sandstone initially contains a significant amount of K-feldspar (5 vol%, Scenario 7), the lowest pH attained is 5.1, with a final mineral assemblage of quartz, K-feldspar and illite, without kaolinite (Fig. 7G). If the diagenetic temperature is set to 200°C, the minimum pH decreases to 3.0 (Scenario 8, Fig. 7H). Conversely, if the diagenetic temperature is set to 80°C, the minimum pH increases to 3.6 (Scenario 9, Fig. 7I).

The modeling results consistently show that at high fluid/rock mass ratios, where only a small amount of sandstone reacts with 1 kg of brine, pH remains above 5, and the brine is in equilibrium with K-feldspar or albite (Fig. 7A-I). This suggests that at high fluid/rock mass ratios, kaolinite originally in the sandstone is completely dissolved, while K-

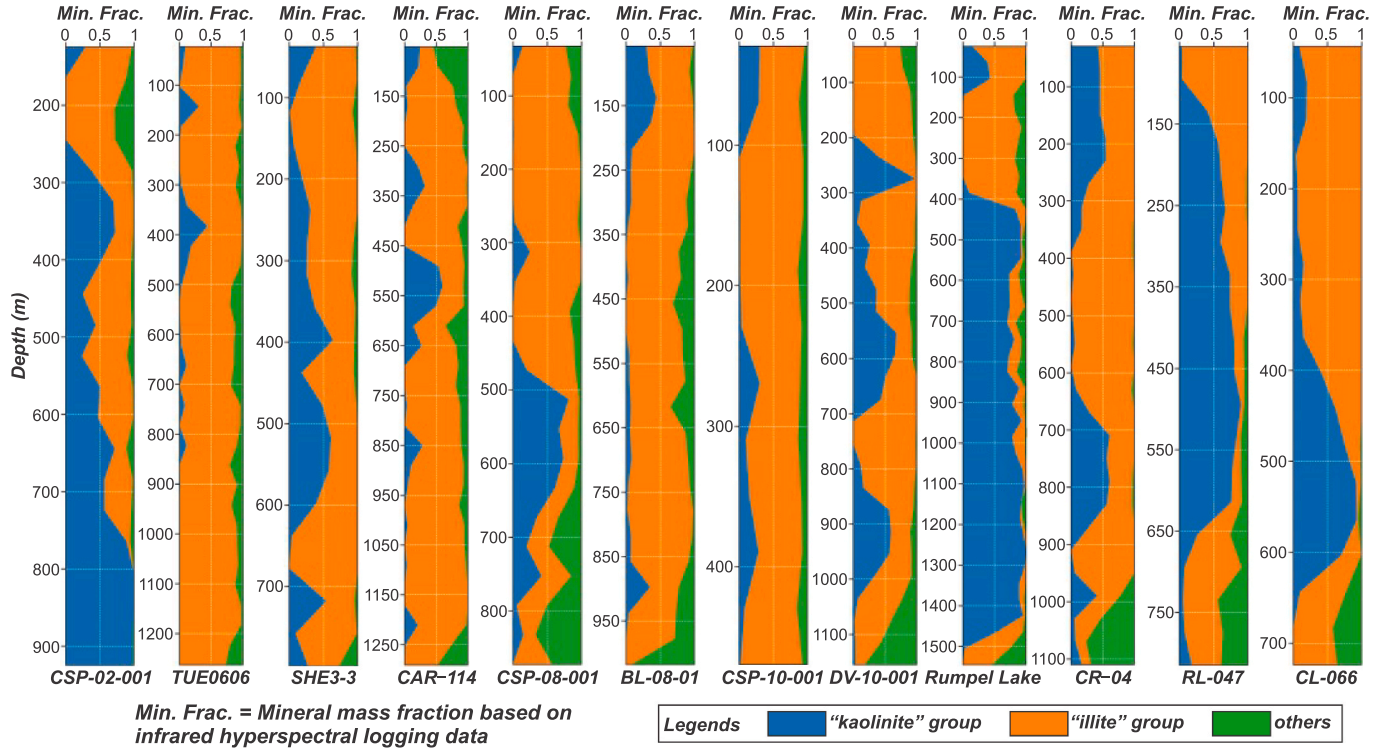

Fig. 5. Distribution of grouped clay minerals in 12 drill cores across the Athabasca Basin, based on infrared hyperspectral logging data from Bosman and Percival (2014) and Percival et al. (2018). Note kaolinite of varying crystallinity is grouped with dickite as "kaolinite", illite is combined with white mica and labeled as "illite", and the remaining minerals are combined as "others". All drillholes (locations shown in Fig. 2A) reach the basal unconformity, except CSP-02–001 and CSP-08–001.

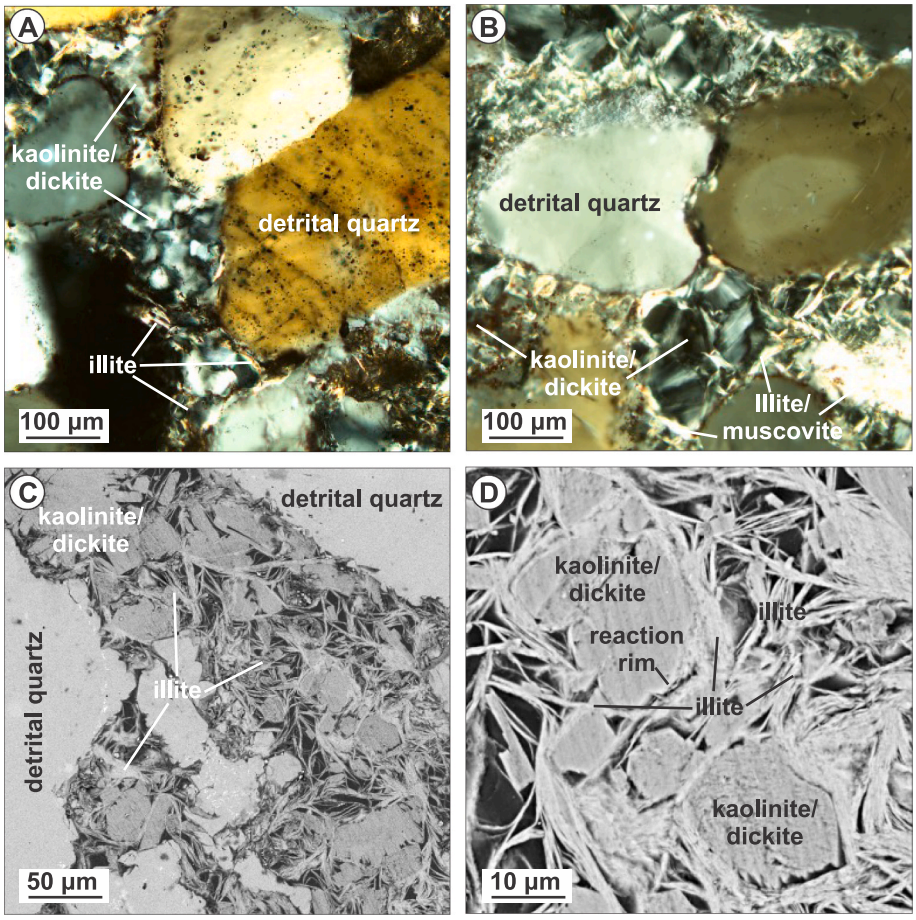

Fig. 6. (A, B) Cross-polarized petrographic photos showing kaolinite/dickite coexisting with illite in the interstitial space between detrital quartz grains. (C, D) SEM images showing illite coexisting, crosscutting, and replacing pre-existing kaolinite/dickite. Note the interweaving relationship between illite and kaolinite/dickite and local development of reaction rims of illite around kaolinite/dickite.

feldspar or albite precipitates by using K^+ or Na^+ from the brine. Conversely, at low fluid/rock mass ratios, pH is decreased, and the fluid equilibrates with both kaolinite and illite (Fig. 7A-I). The lowest pH values reached are mostly < 3.5, except when K concentrations in the fluid are low (e.g., K = 1,000 ppm, pH = 4.4, Scenario 2) or K-feldspar content in the sandstone is high (e.g., K-feldspar = 5 vol%, pH = 5.1, Scenario 7).

5. Discussion

5.1. Mechanisms and conditions of basin-scale generation of hyperacidic brines

Based on the infrared hyperspectral logging data and petrographic observations indicating the basin-wide coexistence of kaolinite and illite in quartz-dominated sandstones (Figs. 5 and 6), and fluid inclusion data indicating high concentrations of K in basinal brines in the Athabasca Basin (Fig. 4), we propose that the basin-scale development of hyperacidic brines resulted from pervasive reactions between K-rich brines and kaolinite, as shown by the reaction equation below:

$$3\text{kaolinite } [Al_2Si_2O_5(OH)_4] + 2\ K^+ \leftrightarrow 2\text{illite } [KAl_3Si_3O_{10}(OH)_2] + 3H_2O + 2H^+$$

The geochemical modeling results presented in this study (Fig. 7) clearly indicate that hyperacidic brines with pH below 3.5 can be produced from an originally circumneutral brine with a pH of 6 through fluid-rock interaction in sandstone-dominated sedimentary basins. The necessary conditions for this to occur include high concentrations of K in the original brine, a dominance of detrital quartz with low content or absence of feldspar in the sandstone, the presence of kaolinite in the original sandstone, and relatively low fluid/rock mass ratios. It can be demonstrated that all these conditions for the generation of hyperacidic brines were satisfied through sedimentary and diagenetic processes in the Athabasca Basin, as summarized in Fig. 8 and discussed below.

The fluviatile sandstones that constitute the bulk of the basin infill are predominantly composed of compositionally and texturally mature, quartz-dominated, feldspar-poor detrital clasts, together with minor amounts of clay minerals, mainly kaolinite. These detrital clasts were derived from provenance areas that experienced intense chemical weathering and were subsequently deposited in continental fluvial environments (Ramaekers et al., 2007; Fig. 8A). The intense chemical weathering of feldspar and other silicate minerals into kaolinite-dominated clays in the source region was likely facilitated by the relatively high concentrations of $CO_2(g)$ in the Proterozoic atmosphere compared to modern levels (Halevy and Bachan, 2017). The chemical weathering was further enhanced by the tropical and humid climate during the deposition of fluviatile sedimentary rocks in the Athabasca Basin, as evidenced by the extensive development of iron oxide (hematite) minerals in the sandstones and the paleoregolith profiles immediately below the basin (Jefferson et al., 2007).

During the deposition of the marine carbonates in the Carswell Formation and the overlying eroded evaporite deposits (Fig. 2B), large amounts of K-rich brines likely formed through intense seawater evaporation beyond the saturation point of halite, with some approaching sylvite saturation (Fig. 4; Fontes and Matray, 1993; Richard et al., 2011). This marks a significant paleoclimatic transition from the tropical, humid conditions for the deposition of fluviatile sandstones and

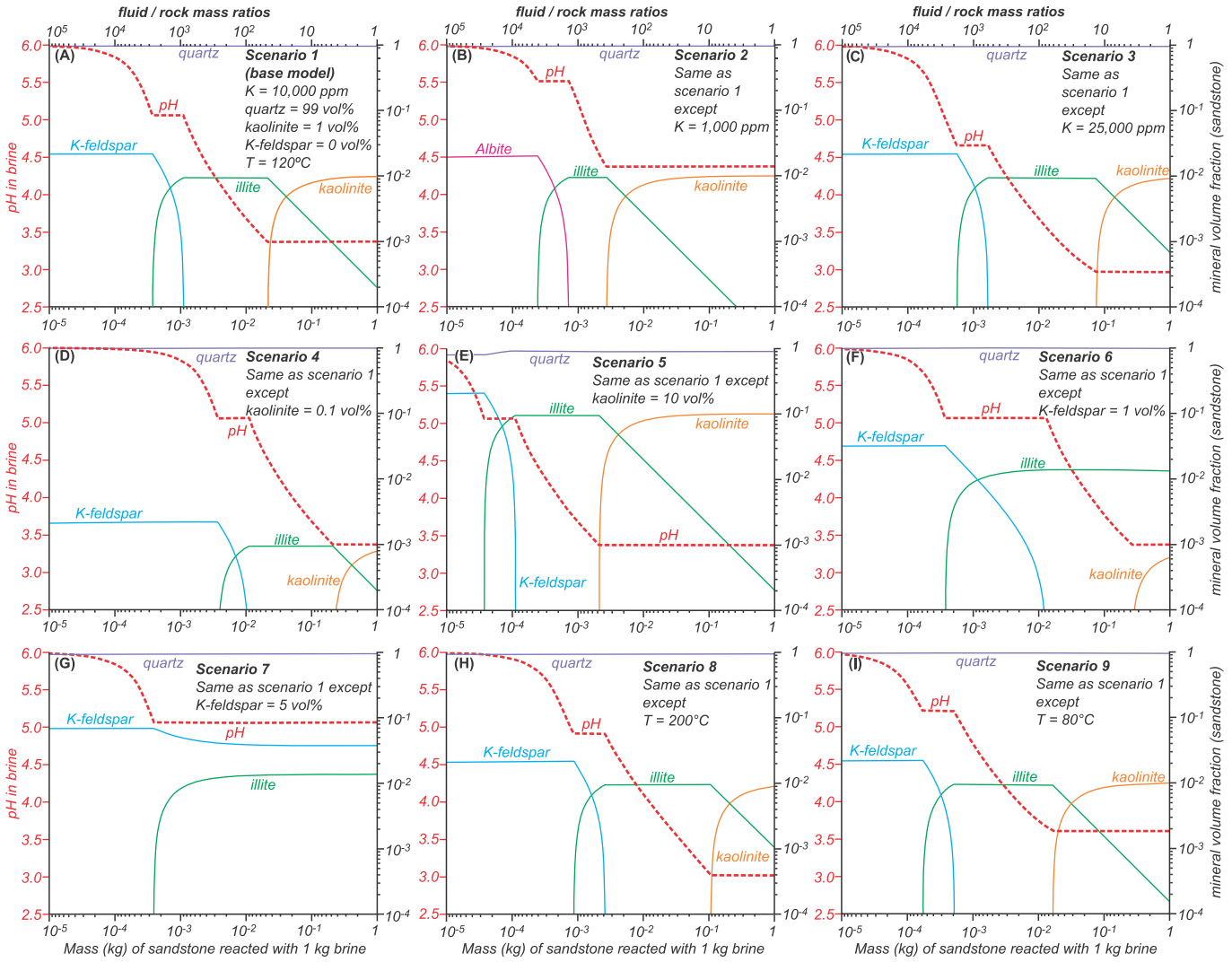

Fig. 7. Modeling results of Scenario 1 to 9 (A to I) showing the variation of pH and mineral volume fraction as a function of mass (kg) of sandstone reacting with 1 kg brine, with corresponding fluid/rock mass ratios from 10^5 to 1.

lacustrine mudstones (from the Fair Point Group to the Douglas Formation) to the subtropical, arid conditions for the deposition of marine carbonates and evaporites of the Carswell Formation (Ramaekers et al., 2007; Richard et al., 2011). The K-rich brines produced at the surface subsequently descended due to their high density, infiltrating the underlying quartz-dominated, kaolinite-bearing fluviatile sandstone lithostratigraphic packages (Fig. 8B). Their migration was likely channeled through structural or lithostratigraphic windows with relatively high permeabilities within the mudstone-bearing interlayers of the Douglas Formation and Wolverine Point Group. The most probable flow pathways are intra-basinal faults that breached these mud-rich aquitards, with such faults likely best developed in areas above regional basement fault zones, such as WMTZ, STZ, CWS, and GRSZ shown in Fig. 2A (Ramaekers et al., 2007; Kitchen, 2022). The influence of major basement faults on structures within the basin is reflected by isopach maps of the stratigraphic units (Ramaekers et al., 2007, 2017; Maxeiner et al., 2021) as well as seismic reflection data indicating reactivated basement-rooted faults propagating into the sedimentary cover (Hajnal et al., 2010).

Once the K-rich brines infiltrated into sandstone aquifers, they formed plumes that spread laterally (Fig. 8B). The brines gradually mixed with the original pore water (meteoric) and, facilitated by fluid convection, finally replaced the original pore water (Fig. 8C). At the same time, the K-rich brines extensively reacted with kaolinite to form illite and released H^+, through the fluid-rock reaction shown above (Fig. 8C). This reaction was facilitated by elevated burial temperature (>120°C) (Berger et al., 1997) and fluid convection, which homogenizes the composition of pore fluids. Fluid convection in the Athabasca Basin has been demonstrated to be viable through numerical modeling of fluid flow (Raffensperger and Garven, 1995; Li et al., 2016) and is reflected by a basin-scale quartz dissolution-precipitation pattern identified by petrographic studies and supported by reactive mass transport modeling (Wang et al., 2021). The multi-pass nature of fluid convection implicates low fluid/rock mass ratios, because a specific volume of fluid can repeatedly interact with a given volume of sandstone if convection persists (Wang et al., 2021). Additionally, the intense evaporation required to generate K-rich brines necessitates the removal of ~ 90.6 % (halite saturation) to ~ 99.4 % (sylvite saturation) of the original seawater (McCaffrey et al., 1987; Fontes and Matray, 1993), further supporting a low fluid/rock mass ratio. Geochemical path modeling shows that only low fluid/rock mass ratios are favorable for achieving low pH values, allowing an excess of kaolinite relative to K-rich brines to produce illite and H^+ (Fig. 7). Once the equilibrium between kaolinite and illite is achieved through the above-discussed reaction, the low pH of the brines remains stable, as demonstrated by the geochemical path modeling results (Fig. 7). However, although kaolinite-illite equilibrium is suggested by the ubiquitous coexistence of the two minerals and the interweaving and reaction-rim textures between them (Fig. 6), it does

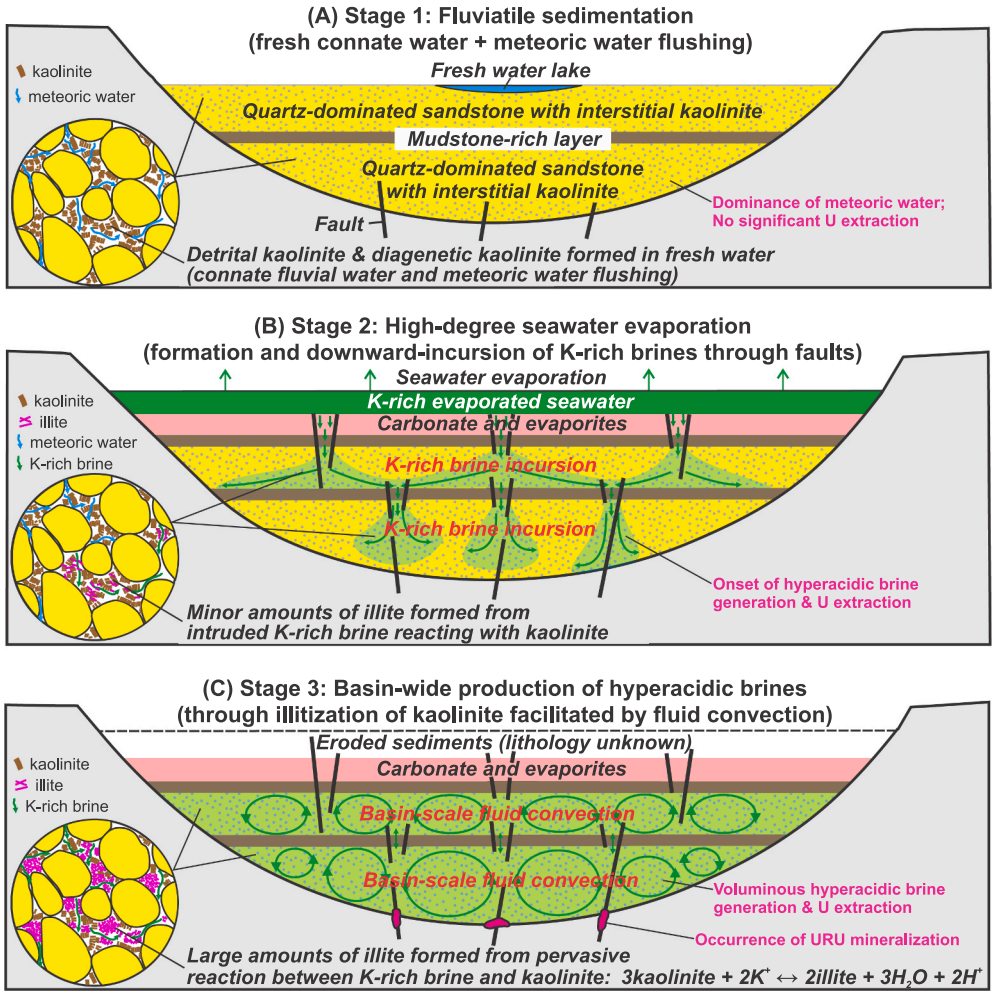

Fig. 8. Conceptual model of the development processes of hyperacidic brines in the Athabasca Basin, highlighting three key stages. (A) Deposition of quartz-dominated sandstone with interstitial kaolinite in a freshwater environment as the starting condition. (B) Formation of K-rich brines through intense seawater evaporation and their infiltration into sandstone successions. (C) Reaction between K-rich brines and kaolinite to form illite and release acid, which facilitates U extraction and mineralization.

not mean that all kaolinite in the sandstone was in equilibrium with the brine and illite. The kaolinite and dickite with δD-$\delta^{18}O$ isotope signatures indicating a supergene chemical weathering origin (Quirt, 2001) may have escaped the reaction with the K-rich brines. However, large amounts of hyperacidic brines could still be produced if K-rich brines interacted with sufficient amounts of kaolinite/dickite within the sandstone. It is important to note that despite the intensive fluid-rock interactions discussed above, the high fO_2 in the evaporated seawater due to dissolved atmospheric O_2 (g) may be largely retained, because the sandstone is dominantly composed of quartz and lacks minerals that contain significant amounts of reducing agents (e.g., Fe^{2+}). This, coupled with the hyperacidic nature of the brines, facilitates the leaching of uranium from detrital minerals and contributes to subsequent uranium mineralization.

5.2. *Implications for mineralization of U and other metals in sedimentary basins*

Based on the study of the Athabasca Basin, three fundamental conditions are required for the generation and preservation of voluminous hyperacidic brines in sedimentary basins. The first one is the development of thick successions of compositionally mature sandstones, with quartz as the dominant framework mineral and feldspar being negligible, and kaolinite as the dominant mineral filling the interstitial space. The second condition is the development of K-rich brines, which generally requires seawater evaporation beyond the halite saturation point. The third condition is relatively low fluid/rock mass ratios, which facilitate the equilibrium of the diagenetic reaction between kaolinite and K-rich brine to form illite and ultimately control pH. While the first condition can be examined through systematic core logging and petrographic studies of sandstones, the second condition may be evaluated based on data from evaporites, formation water and fluid inclusions. The third condition for the development of hyperacidic brines, i.e., low fluid/rock mass ratios, is relatively difficult to evaluate. However, based on the example of the Athabasca Basin, a hydrostratigraphic configuration with thick sandstone packages (aquifers) sandwiched between mudstone-bearing intervals (aquitards) may be considered favorable for keeping fluid/rock mass ratios low, which is also consistent with the development of multi-pass fluid convection (Wang et al., 2021). While any one of these favorable conditions may exist in sedimentary basins at a given time, the coexistence of all three is relatively rare, which may explain why hyperacidic brines are not commonly preserved. Consequently, recognition of the combination of all these favorable conditions is highly valuable for understanding why certain sedimentary basins are exceptionally enriched in certain resources (e.g., U in the Athabasca Basin) or for predicting whether other basins have the potential for holding similar resources.

It is interesting to note that a global compilation of compositional

data of saline fluids in modern sedimentary basins shows a distinct negative correlation between K concentrations and pH values: as the K concentration increases from 1,000 to 20,000 mg/L, the pH of the brines decreases from 6 to 3.5 (Hanor, 1994). As K-rich brines are commonly developed through seawater evaporation beyond halite saturation toward sylvite saturation (McCaffrey et al., 1987; Fontes and Matray, 1993), the development of evaporites beyond halite saturation may be considered as a favorable condition for the generation of hyperacidic brines. However, the development of K-rich brines alone is insufficient for the formation of hyperacidic brines, which can be demonstrated by counterexamples such as the Paleozoic Williston Basin. This basin, located a few hundred kilometers south of the Athabasca Basin, hosts one of the largest potash resources in the world (Broughton, 2019), implicating that large amounts of K-rich brines were once developed in the basin. However, the pH values of the basinal brines are mostly between 6.2 and 8.1 (Peterman and Thamke, 2016). The lack of hyperacidic brines in this basin is likely due to the abundance of marine carbonate rocks, which act as pH buffers by consuming H^+. This may be a key reason for explaining why there is no U mineralization here, despite a portion of the basement rocks underlying the Williston Basin is the same as those underlying the U-rich Athabasca Basin, i.e., belonging to the Hearne and Rae cratons of the Churchill Province (Hoffman, 1988).

The critical role of hyperacidic brines in the formation of high-grade U deposits can be further demonstrated by comparing the Athabasca Basin with other Proterozoic basins with known URU mineralization, especially the Thelon Basin in Canada and the Kombolgie Basin in northern Australia (Jefferson et al., 2007; Kyser and Cuney, 2015). The Thelon Basin, located ~ 900 km northeast of the Athabasca Basin, is strikingly similar to the Athabasca Basin in terms of age, tectonic setting, and basin fill (dominated by fluviatile sandstones). However, while the Thelon Basin also hosts significant URU deposits, they are smaller and of lower grade than those in the Athabasca Basin (Jefferson et al., 2007). This difference is likely related to a subtle difference in sandstone lithology between the two basins: while only rare feldspar grains are preserved in the Athabasca Basin sandstones, the Thelon Basin sandstones contain 1–5 vol% K-feldspar (Jefferson et al., 2007; Hiatt et al., 2010). Based on our geochemical modeling results (Fig. 7G), the presence of even minor amounts of K-feldspar (5 vol%) would prevent the formation of hyperacidic brines with pH < 3.5. Therefore, the relatively small-scale and low-grade URU mineralization in the Thelon Basin (Fig. 1A) may be due to the limited or poor development of hyperacidic brines.

Similarly, the Paleo- to Mesoproterozoic Kombolgie Basin in northern Australia, which is part of the larger McArthur Basin, hosts several URU deposits that are comparable to those in the Athabasca Basin in terms of metal tonnage but at much lower grades (Fig. 1a). It is interesting to note that the stratigraphic succession of the Kombolgie Basin (the Kombolgie Subgroup) is similar to that in the Athabasca Basin. It comprises thick packages of coarse-grained siliciclastic rocks of fluvial facies, followed by finer-grained distal fluvial and lacustrine facies, and finally interbedded marine and eolian facies, with a distinctive middle interval that is marked by mud-rich, fine-grained sandstones and mud-cracked siltstones representing tidal deposition, and a top interval that contains halite casts, gypsum nodules, stromatolites, and phosphate (Hiatt et al., 2021). However, like the siliciclastic rocks in the Thelon Basin, those in the Kombolgie Basin contain feldspar in sandstones and polymict conglomerates (Hiatt et al., 2021), which may have resulted in less development of hyperacidic brines and consequently lower-grade U mineralization compared to the Athabasca Basin. It is noteworthy that URU deposits are rarely found outside the Kombolgie Basin in the larger McArthur Basin, where carbonates and feldspar are abundant at various stratigraphic levels (Polito et al., 2006), which may have hampered the basin-scale development of hyperacidic brines throughout the McArthur Basin, thereby restricting the formation of URU deposits only to the Kombolgie Basin.

The implications of hyperacidic brines for mineralization may be further extended to other types of mineral deposits in sedimentary basins. Ore-forming fluids with low pH values between 3 and 6 have been inferred for many important basin-hosted mineral deposits, including Mississippi Valley-type (MVT) Zn-Pb (Anderson and Macqueen, 1988; Corbella et al., 2004), sedimentary-exhalative (SEDEX) or clastic-dominated (CD-type) Zn-Pb (Cooke et al., 2000; Leach et al., 2010; Spinks et al., 2022), and sediment-hosted stratiform Cu (Co) (Hitzmann et al., 2010; Williams-Jones and Vasyukova, 2022). Some studies suggest that ore-forming fluids for sediment-hosted Zn-Pb deposits were hyperacidic, with pH values below 3.5, such as ~ 2 (Liu et al., 2021) or 2.8–4.2 (Cooke et al., 2000). The acidic nature of these fluids is consistent with the widespread development of carbonate dissolution features in MVT and SEDEX or CD-type deposits (Anderson and Macqueen, 1988; Leach et al., 2005, 2010). Several studies also indicate that K-rich basinal brines were involved in the formation of MVT and Sedex Zn-Pb deposits (Viet and Leach, 1990; Wilkinson et al., 2009), and sediment-hosted stratiform Cu-Co deposits (Davey et al., 2020). However, unlike URU deposits that appear to be exclusively associated with quartz-dominated sedimentary successions, the Zn-Pb-Cu mineralization can develop in basins with abundant carbonates and feldspar. Understanding the mechanisms behind these subtle differences in the geological and geochemical conditions favorable for U and Zn-Pb-Cu mineralization in sedimentary basins is critical for identifying ore-controlling factors and warrants further investigation.

6. Conclusions

A key reason why most high-grade and large-tonnage unconformity-related uranium (URU) deposits in the world are concentrated in a few Proterozoic sedimentary basins is revealed in this study by geochemical reaction path modeling based on petrographic, infrared hyperspectral logging, and fluid inclusion data from the Athabasca Basin. It is shown that the development of voluminous oxidizing, hyperacidic (pH < 3.5) basinal brines capable of dissolving high concentrations of U (up to 3700 ppm) is critical for the formation of large numbers of high-grade URU deposits. These hyperacidic brines were generated on a basin-wide scale through diagenetic reactions between K-rich brines and kaolinite-bearing, quartz-dominated sandstones with rare or no feldspar. The incursion of K-rich brines derived from seawater evaporation into the underlying fluviatile sandstones caused basin-wide illitization of kaolin group minerals, resulting in pH decrease via the reaction: 3kaolinite $[Al_2Si_2O_5(OH)_4] + 2\,K^+ \leftrightarrow$ 2illite $[KAl_3Si_3O_{10}(OH)_2] + 3H_2O + 2H^+$. The abundance of hyperacidic brines, combined with their high oxygen fugacity inherited from the evaporated seawater, facilitated U extraction from U-bearing detrital minerals, leading to the development of large volumes of U-rich brines, which contribute to the formation of exceptionally rich and large URU deposits in the Athabasca Basin. The conditions for basin-scale development of hyperacidic brines as identified in this study, including thick successions of quartz-dominated, kaolinite-bearing, feldspar-poor sandstones, K-rich brines from seawater evaporation, and low fluid/rock mass ratios, have important implications for evaluating the potential of high-grade, large-tonnage U resources in sedimentary basins and their exploration.

CRediT authorship contribution statement

Yumeng Wang: Writing – review & editing, Writing – original draft, Visualization, Validation, Software, Methodology, Investigation, Formal analysis, Data curation, Conceptualization. **Guoxiang Chi:** Writing – review & editing, Visualization, Validation, Supervision, Software, Resources, Project administration, Methodology, Investigation, Funding acquisition, Formal analysis, Data curation, Conceptualization. **Sean A. Bosman:** Writing – review & editing, Resources, Methodology, Investigation, Data curation.

Data availability

The original dataset for K-Cl concentrations from fluid inclusion LA-ICP-MS analyses of diagenetic fluids and ore-forming fluids in the Athabasca Basin, K and Cl concentrations during seawater evaporation, and hyperspectral logging of drill cores in the Athabasca Basin used in this paper are available in Wang et al. (2025), "Basin-scale production of hyperacidic brines is critical for the formation of high-grade and large-tonnage uranium deposits in sedimentary basins", Mendeley Data, V2, https://doi.org/10.17632/ybjgyz6hxz.3.

Declaration of competing interest

The authors declare that they have no known competing financial interests or personal relationships that could have appeared to influence the work reported in this paper.

Acknowledgements

This study was supported by NSERC Discovery Grants (RGPIN-2018-06458, RGPIN-2024-05959). The authors sincerely thank Associate Editor Dr. Benjamin Tutolo, Executive Editor Dr. Hailiang Dong, and Dr. Jeffrey Catalano for their editorial handling and valuable feedback. We also extend our deep gratitude to Dr. Steve Beyer and the two anonymous reviewers for their thorough reviews and constructive suggestions, which have greatly contributed to improving the quality of this manuscript.

Appendix A. Supplementary material

This file is the Supplementary Material (SM) for the manuscript GCA-D-24–01080 submitted to Geochimica et Cosmochimica Acta. This file contains the compiled K-Cl concentration data from fluid inclusion LA-ICP-MS analyses of diagenetic fluids and ore-forming fluids in the Athabasca Basin, published up to the time of manuscript submission (compiled from Richard et al., 2016; Chi et al., 2019; Martz et al., 2019; Rabiei et al., 2023; Ferguson et al., 2025). These data are presented in SM Table S1 and are used in Fig. 4 to illustrate the correlation between K and Cl concentrations. SM Table S2 shows data on K and Cl concentrations during seawater evaporation (from Fontes and Matry, 1993), which is used to delineate the typical reaction path for K-Cl concentrations variations during seawater evaporation. This file also includes detailed information on the dataset of raw infrared hyperspectral logging data for sedimentary rocks in the Athabasca Basin (Bosman and Percival, 2014; Percival et al., 2018). SM Table S3 presents the processed data on the relative abundances of kaolinite, illite, and other minerals, obtained using the binning method with a 40-meter interval.

Supplementary material to this article can be found online at https://doi.org/10.1016/j.gca.2025.03.031.

References

Adlakha, E.E., Hattori, K., 2021. Thermotectonic events recorded by U-Pb geochronology and Zr-in-rutile thermometry of Ti oxides in basement rocks along the P2 fault, eastern Athabasca Basin, Saskatchewan, Canada. GSA Bull. 134, 567–576.

Alexandre, P., Kyser, T.K., Thomas, D., Polio, P., Marlat, J., 2009. Geochronology of unconformity-related uranium deposits in the Athabasca Basin, Saskatchewan, Canada and their integration in the evolution of the basin. Mineral. Deposita 44, 41–59.

Anderson, G.M., Macqueen, R.W., 1988. Mississippi Valley-type lead-zinc deposits. In: Ore Deposit Models (Eds. R.G. Roberts and P.A. Sheahan), Geoscience Canada Reprint Series 3, 73−90.

Berger, G., Lacharpagne, J.-C., Velde, B., Beaufort, D., Lanson, B., 1997. Kinetic constraints on illitization reactions and the effects of organic diagenesis in sandstone/shale sequences. Appl. Geochem. 12, 23–35.

Bethke, C.M., 2022. Geochemical and biogeochemical reaction modeling (Third Edition). Cambridge University Press, Cambridge, UK, p. 502.

Bosman, S.A., Percival, J.B., 2014. Spectral reflectance data and interpretation of Athabasca Basin drillholes, Saskatchewan (NTS 64L, 74F to 74K, and 74N to 74P). Saskatchewan Geological Survey, Data File Report D34. http://publications.gov.sk.ca/details.cfm?p=82130.

Bosman, S.A., Ramaekers, P., 2015. Athabasca Group + Martin Group = Athabasca Supergroup? Athabasca Basin multiparameter drill log compilation and interpretation, with updated geological map. In: Summary of Investigations 2015. In: Saskatchewan Geological Survey, vol. 2. Sask. Ministry of Economy, Misc. Rep. 2015-4.2, Paper A-5, 13 pp.

Bowen, B.B., Martini, B.A., Chan, M.A., Parry, W.T., 2007. Reflectance spectroscopic mapping of diagenetic heterogeneities and fluid-flow pathways in the Jurassic Navajo Sandstone. Am. Assoc. Pet. Geol. Bull. 91, 173–190.

Broughton, P.L., 2019. Economic geology of southern Saskatchewan potash mines. Ore Geol. Rev. 133, 103117.

Card, C.D., Bethune, K.M., Rayner, N., Ashton, K.E., 2021. Tectonic significance of the Virgin River Shear Zone of the Canadian Shield and implications for the origin of the Snowbird Tectonic Zone of Laurentia. Precam. Res. 361, 106241.

Chi, G., Li, Z., Chu, H., Bethune, K.M., Quirt, D.H., Ledru, P., Normand, C., Card, C., Bosman, S., Davis, W.J., Potter, E.G., 2018. A shallow-burial mineralization model for the unconformity-related uranium deposits in the Athabasca Basin. Econ. Geol. 113, 1209–1217.

Chi, G., Chu, H., Petts, D., Potter, E., Jackson, S., Williams-Jones, A., 2019. Uranium-rich diagenetic fluids provide the key to unconformity-related uranium mineralization in the Athabasca Basin. Sci. Rep. 2019 (5530), 1–10.

Chu, H., Chi, G., 2016. Thermal profiles inferred from fluid inclusion and illite geothermometry from sandstones of the Athabasca basin: Implications for fluid flow and unconformity-related uranium mineralization. Ore Geol. Rev. 75, 284–303.

Chu, H., Chi, G., Bosman, S., Card, C., 2015. Diagenetic and geochemical studies of sandstones from drill core DV10-001 in the Athabasca Basin, Canada, and implications for uranium mineralization. J. Geochem. Explor. 148, 206–230.

Cooke, D.R., Bull, S.W., Large, R.R., McGoldrick, P.J., 2000. The importance of oxidized brines for the formation of Australian Proterozoic stratiform sediment-hosted Pb-Zn (Sedex) deposits. Econ. Geol. 95, 1–16.

Corbella, M., Ayora, C., Cardellach, E., 2004. Hydrothermal mixing, carbonate dissolution and sulfide precipitation in Mississippi Valley-type deposits. Mineral. Deposita 39, 344–357.

Creaser, R.A., Stasiuk, L.D., 2007. Depositional age of the Douglas Formation, northern Saskatchewan, determined by Re-Os geochronology. Geol. Surv. Can. Bull. 588, 341–346.

Dargent, M., Dubessy, J., Truche, L., Bazarkina, E.F., Nguyen-Trung, C., Robert, P., 2013. Experimental study of uranyl (VI) chloride complex formation in acidic LiCl aqueous solutions under hydrothermal conditions (T = 21℃-350℃, Psat) using Raman spectroscopy. Eur. J. Mineral. 25, 765–775.

Dargent, M., Truche, L., Dubessy, J., Bessaque, G., Marmier, H., 2015. Reduction kinetics of aqueous U(VI) in acidic chloride brines to uraninite by methane, hydrogen or C-graphite under hydrothermal conditions: Implications for the genesis of unconformity-related uranium ore deposits. Geochim. Cosmochim. Acta 167, 11–26.

Davey, J., Roberts, S., Wilkinson, J.J., 2020. Copper- and cobalt-rich, ultrapotassic bittern brines responsible for the formation of the Nkana-Mindola deposits, Zambian Copperbelt. Geology 49, 341–345.

Deng, T., Chi, G., Williams-Jones, A.E., Li, Z., Wang, Y., Xu, D., Wang, Z., 2023. Re-evaluation of equilibrium relationships involving U^{6+}/U^{4+} and Fe^{3+}/Fe^{2+} in hydrothermal fluids and their implications for U mineralization. Chem. Geol. 625, 121432.

Derome, D., Cathelineau, M., Cuney, M., Fabre, C., Lhomme, T., Banks, D.A., 2005. Mixing of sodic and calcic brines and uranium deposition at McArthur River, Saskatchewan, Canada: a Raman and laser-induced breakdown spectroscopic study of fluid inclusions. Econ. Geol. 100, 1529–1545.

Ferguson, D., Chi, G., Normand, C., Mercadier, J., Wang, Y., McKee, K., Anderson, M., Robbins, J., 2025. Relationship between U and Ni-Co-As mineralization in the Midwest polymetallic U deposit, Athabasca Basin (Canada) – constraints from mineralogical, geochemical, and fluid inclusion studies. Mineral. Deposita 60, 63–83.

Fontes, J.C., Matray, J.M., 1993. Geochemistry and origin of formation brines from the Paris Basin, France 1. Brines associated with Triassic salts. Chem. Geol. 109, 149–175.

Gaboreau, S., Cuney, M., Quirt, D., Beaufort, D., Patrier, P., Mathieu, R., 2007. Significance of aluminum phosphate-sulfate minerals associated with U unconformity-type deposits: The Athabasca Basin. Canada. Am. Mineral. 92, 267–280.

Hajnal, Z., White, D.J., Takacs, E., Gyorfi, I., Annesley, I.R., Wood, G., O'Dowd, C., Nimeck, G., 2010. Application of modern 2-D and 3-D seismic-reflection techniques for uranium exploration in the Athabasca Basin. Can. J. Earth Sci. 47, 761–782.

Halevy, I., Bachan, A., 2017. The geologic history of seawater pH. Science 355, 1069–1071.

Hanor, J.S., 1994. Origin of saline fluids in sedimentary basins. Geol. Soc. London, Special Pub. 78, 151–174.

Hiatt, E.E., Palmer, S.E., Kyser, T.K., O'Connor, T.K., 2010. Basin evolution, diagenesis and uranium mineralization in the Paleoproterozoic Thelon Basin, Nunavut. Canada. Basin Res. 22, 302–323.

Hiatt, E.E., Kyser, T.K., Polito, P.A., Marlett, J., Pufahl, P., 2021. The Paleoproterozoic Kombolgie Subgroup (1.8 Ga), McArthur Basin, Australia: sequence stratigraphy, basin evolution, and unconformity-related uranium deposits following the Great Oxidation Event. Can. Mineral. 59, 1049–1083.

Hitzman, M.W., Selley, D., Bull, S., 2010. Formation of sedimentary rock-hosted stratiform copper deposits through Earth history. Econ. Geol. 105, 627–639.

Hoffman, P.F., 1988. United plates of America, the birth of a craton: Early Proterozoic assembly and growth of Laurentia. Ann. Rev. Earth Planet. Sci. 16, 543–603.

Hoeve, J., Quirt, D.H., 1984. Mineralization and host rock alteration in relation to clay mineral diagenesis and evolution of the Middle-Proterozoic, Athabasca Basin, northern Saskatchewan, Canada. Technical Report 187 Saskatchewan Research Council. 187 pp.

Hoeve, J., Sibbald, T.I.I., 1978. On the genesis of Rabbit Lake and other unconformity-type uranium deposits in northern Saskatchewan. Canada. Econ. Geol. 73, 1450–1473.

IAEA (International Atomic Energy Agency), 2018. Geological Classification of Uranium Deposits and Description of Selected Examples, IAEA-TECDOC-1842, p. 417.

Jefferson, C.W., Thomas, D.J., Gandhi, S.S., Ramaekers, P., Delaney, G., Brisbin, D., Cutts, C., Portella, P., Olson, R.A., 2007. Unconformity-related uranium deposits of the athabasca basin, saskatchewan and alberta. Geol. Surv. Can. Bull. 588, 23–67.

Kalintsev, A., Migdisov, A., Alcorn, C., Baker, J., Brugger, J., Mayanovic, R.A., Akram, N., Guo, X., Xu, H., Boukhalfa, H., Caporuscio, F.A., Viswanathan, H., Jove-Colon, C., Wang, Y., Matteo, E., Roback, R., 2021. Uranium carbonate complexes demonstrate drastic decrease in stability at elevated temperatures. Commun. Chem. 4 (120), 1–8.

Kister, P., Vieillard, P., Cuney, M., Quirt, D., Laverret, E., 2005. Thermodynamic constraints on the mineralogy and fluid composition evolution in a clastic sedimentary basin: the Athabasca Basin (Saskatchewan, Canada). Eur. J. Mineral. 17, 325–342.

Kitchen, A.T., 2022. Deformation bands and their relationship to syn- to post-Athabasca faulting and unconformity-related uranium deposits: A case study of the C1 fault corridor and WS shear zone (Gryphon and Phoenix deposits) in the eastern Athabasca Basin. University of Regina, M.Sc. Thesis, p. 216.

Komninou, A., Sverjensky, D.A., 1996. Geochemical modeling of the formation of an unconformity-type uranium deposit. Econ. Geol. 91, 590–606.

Kotzer, T.G., Kyser, T.K., 1995. Petrogenesis of the Proterozoic Athabasca Basin, northern Saskatchewan, Canada, and its relation to diagenesis, hydrothermal uranium mineralization and paleohydrogeology. Chem. Geol. 120, 45–89.

Kyser, K., Cuney, M., 2015. Basins and uranium deposits: In: Geology and Geochemistry of Uranium and Thorium Deposits. In: Mineralogical Association of Canada Short Course Series 46, pp. 224–250.

Leach, D.L., Sangster, D.F., Kelley, K.D., Large, R.R., Garven, G., Allen, C.R., Gutzmer, J., Walters, S., 2005. Sediment-hosted lead-zinc deposits: a global perspective. In: One Hundredth Anniversary Volume, Society of Economic Geologists, pp. 561−607.

Leach, D.L., Bradley, D.C., Huston, D., Pisarevsky, S.A., Taylor, R.D., Gardoll, S.J., 2010. Sediment-hosted lead-zinc deposits in Earth history. Econ. Geol. 105, 593–625.

Li, Z., Chi, G., Bethune, K.M., 2016. The effects of basement faults on thermal convection and implications for the formation of unconformity-related uranium deposits in the Athabasca Basin, Canada. Geofluids 16, 729–751.

Liu, W., Spinks, S.C., Glenn, M., MacRae, C., Pearce, M.A., 2021. How carbonate dissolution facilitates sediment-hosted Zn-Pb mineralization. Geology 49, 1363–1368.

Mason, B., Moore, C.B., 1982. Principles of geochemistry, Fourth edition. John Wiley and Sons, New York. p, p. 344.

Martz, P., Mercadier, J., Cathelineau, M., Boiron, M.C., Quirt, D., Doney, A., Gerbeaud, O., Wally, E.D., Ledru, P., 2019. Formation of U-rich mineralizing fluids through basinal brine migration within basement-hosted shear zones: a large-scale study of the fluid chemistry around the unconformity-related Cigar Lake U deposit (Saskatchewan, Canada). Chem. Geol. 508, 116–143.

Maxeiner, R., Ashton, K.E., Bosman, S., Kohlruss, D., Love, M., Love, T., Marsh, A., Morelli, R., Slimmon, W.L., 2021. Geological map of Saskatchewan; Saskatchewan Geological Survey, Saskatchewan Energy and Resources, scale 1:1 000 000.

McCaffrey, M.A., Lazar, B., Holland, H.D., 1987. The evaporation path of seawater and the coprecipitation of Br^- and K^+ with halite. Jour. Sedim. Petrol. 57, 928–937.

Mercadier, J., Richard, A., Cathelineau, M., 2012. Boron- and magnesium-rich marine brines at the origin of giant unconformity-related uranium deposits: $\delta^{11}B$ evidence from Mg-tourmaline. Geology 40, 231–234.

Migdisov, A.A., Boukhalfa, H., Timofeev, A., Runde, W., Roback, R., Williams-Jones, A. E., 2018. A spectroscopic study of uranyl speciation in chloride-bearing solutions at temperatures up to 250°C. Geochim. Cosmochim. Acta 222, 130–145.

NEA-IAEA, 2023. Uranium 2022: Resources, production and demand. NEA No. 7634, OECD, 561 p.

Okyay, U., Khan, S.D., 2016. Remote detection of fluid-related diagenetic mineralogical variations in the Wingate Sandstone at different spatial and spectral resolutions. Int. J. Appl. Earth Obs. Geoinf. 44, 70–87.

Pagel, M., 1975. Détermination des conditions physico-chimiques de la silicification diagénétique des grès Athabasca (Canada) au moyen des inclusions fluids. C. r. Acad. Sci. Paris 280, 2301–2304.

Peterman, Z., Thamke, J., 2016. Chemical and isotopic changes in Williston Basin brines during long-term oil production: an example from the Poplar dome. Montana. AAPG Bull. 100, 1619–1631.

Percival, J.B., Bosman, S.A., Potter, E.G., Peter, J.M., Laudadio, A.B., Abraham, A.C., Shiley, D.A., Sherry, C., 2018. Customized spectral libraries for effective mineral exploration: mining national mineral collections. Clays Clay Mineral. 66, 297–314.

Polito, P.A., Kyser, T.K., Jackson, M.J., 2006. The role of sandstone diagenesis and aquifer evolution in the formation of uranium and zinc-lead deposits, southern McArthur Basin, Northern Territory. Australia. Econ. Geol. 101, 1189–1209.

Potter, E.G., Kelly, C.J., Davis, W.J., Chi, G., Jiang, S.Y., Rabiei, M., McEwan, B.J., 2022. Fluid sources in basement-hosted unconformity-uranium ore systems: tourmaline chemistry and boron isotopes from the Patterson Lake corridor deposits. Canada. Geochem: Explor. Environ. Anal. 22, geochem2021-037.

Quirt, D.H., 2001. Kaolinite and dickite in the Athabasca sandstone, Northern Saskatchewan, Canada. SRC Publication No. 10400-16D01, 27 pp.

Rabiei, M., Chi, G., Normand, C., Davis, W.J., Fayek, M., Blamey, N.J., 2017. Hydrothermal rare earth element (Xenotime) mineralization at Maw Zone, Athabasca Basin, Canada, and Its Relationship to Unconformity-Related Uranium Deposits. Econ. Geol. 112, 1483–1507.

Rabiei, M., Chi, G., Potter, E., Tschirhart, V., MacKay, C., Frostad, S., McElroy, R., Ashley, R., McEwan, B., 2021. Fluid evolution along the Patterson Lake corridor in the southwestern Athabasca Basin: constraints from fluid inclusions and implications for unconformity-related uranium mineralization. Geochem.: Explor. Environ. Anal., 21, geochem2020-029.

Rabiei, M., Chi, G., Potter, E.G., Petts, D.C., Wang, F., Feng, R., 2023. Spatial variations in fluid composition along structures hosting unconformity-related uranium deposits in the Athabasca Basin, Canada: Implications for ore-controlling factors. Mineral. Deposita 58, 1075–1099.

Raffensperger, J.P., Garven, G., 1995. The formation of unconformity-type uranium ore deposits 1. Coupled groundwater flow and heat transport modeling. Am. J. Sci. 295, 581–636.

Rainbird, R.H., Stern, R.A., Rayner, N., Jefferson, C.W., 2007. Age, provenance, and regional correlation of the Athabasca Group, Saskatchewan and Alberta, constrained by igneous and detrital zircon geochronology. Geol. Surv. Can. Bull. 588, 193–209.

Ramaekers, P., Jefferson, C.W., Yeo, G.M., Collier, B., Long, D.G., Drever, G., McHardy, S., Jiricka, D., Cutts, C., Wheatley, K., Catuneanu, O., Bernier, S., Kupsch, B., Post, R.T., 2007. Revised geological map and stratigraphy of the Athabasca Group, Saskatchewan and Alberta. Geol. Surv. Can. Bull. 588, 155–191.

Ramaekers, P., McElroy, R., Catuneanu, O., 2017. Mid-Proterozoic continental extension as a control on Athabasca region uranium emplacement, Saskatchewan and Alberta, Canada. Mineral Resources to Discover – Proceedings of 14th SGA Meeting (2017) Volume 2, 759–762.

Richard, A., Banks, D.A., Mercadier, J., Boiron, M.C., Cuney, M., Cathelineau, M., 2011. An evaporated seawater origin for the ore-forming brines in unconformity-related uranium deposits (Athabasca Basin): Cl/Br and $\delta^{37}Cl$ analysis of fluid inclusions. Geochim. Cosmochim. Acta 75, 2792–2810.

Richard, A., Rozsypal, C., Mercadier, J., Banks, D.A., Cuney, M., Boiron, M.C., Cathelineau, M., 2012. Giant uranium deposits formed from exceptionally uranium-rich acidic brines. Nat. Geosci. 5, 142–146.

Richard, A., Cathelineau, M., Boiron, M.C., Mercadier, J., Banks, D.A., Cuney, M., 2016. Metal-rich fluid inclusions provide new insights into unconformity-related U deposits (Athabasca Basin and Basement, Canada). Mineral. Deposita 51, 249–270.

Robb, L., 2020. Introduction to ore-forming processes, (2nd edition).

Romberger, S.B., 1984. Transport and Deposition of Uranium in Hydrothermal Systems at Temperatures up to 300 ∘C. Geological Implications. Uranium Geochemistry, Mineralogy, Geology, Exploration and Resources. Springer 12–17.

Scott, R., Chi, G., Bosman, S., 2012. Petrographic characteristics of the Athabasca Group sandstones from the Rumpel Lake drill core, Athabasca Basin, northern Saskatchewan. *In* Summary of Investigations 2012, Volume 2, Saskatchewan Geological Survey, Sask. Ministry of Economy, Misc. Rep. 2012-4.2, Paper A7, 8 p.

Spinks, S.C., Pearce, M.A., Liu, W., Kunzmann, M., Ryan, C.G., Moorhead, G.F., Kirkham, R., Blaikie, T., Sheldon, H.A., Schaubs, P.M., Richard, W.D.A., 2021. Carbonate replacement as the principal ore formation process in the Proterozoic McArthur River (HYC) sediment-hosted Zn-Pb deposit. Australia. Econ. Geol. 116, 693–718.

Viet, J.G., Leach, D.L., 1990. Genetic implications of reginal and temporal trends in ore fluid chemistry of Mississippi valley-type deposits in the Ozark Region. Econ. Geol. 85, 842–861.

Wang, K., Chi, G., Bethune, K.M., Li, Z., Blamey, N., Card, C., Potter, E.G., Liu, Y., 2018. Fluid PTX characteristics and evidence for boiling in the formation of the Phoenix uranium deposit (Athabasca Basin, Canada): Implications for unconformity-related uranium mineralization mechanisms. Ore Geol. Rev. 101, 122–142.

Wang, Y., Chi, G., 2023. Coupling of thermal convection and basin-basement fluid mixing is critical for the formation of unconformity-related uranium deposits: Insights from reactive transport modeling. Chem. Geol. 641 (2023), 121764.

Wang, Y., Chi, G., Li, Z., Bosman, S., 2021. Large-scale thermal convection in sedimentary basins revealed by coupled quartz cementation-dissolution pattern and reactive transport modeling – a case study of the Proterozoic Athabasca Basin (Canada). Earth Planet. Sci. Lett. 574, 117168.

Wang, Y., Chi, G., Ferguson, D., McKee, K., Anderson, M., Robbins, J., 2024. Geochemical modeling of U-Ni-Co-As transport and deposition in acidic basinal brines: implications for unconformity-related U-(Ni-Co-As) mineralization in the Athabasca Basin (Canada). Chem. Geol. 670 (2024), 122456.

Wilkinson, J.J., Stoffell, B., Wilkinson, C.C., Jeffries, T.E., Appold, M.S., 2009. Anomalously metal-rich fluids from hydrothermal ore deposits. Science 323, 764–767.

Williams-Jones, A.E., Vasyukova, O.V., 2022. Constraints on the genesis of cobalt deposits: Part I. Theoretical Considerations. Econ. Geol. 117, 513–528.

Xing, Y., Mei, Y., Etschmann, B., Liu, W., Brugger, J., 2018. Uranium transport in F-Cl-bearing fluids and hydrothermal upgrading of U-Cu ores in IOCG deposits. Geofluids 2018, 1–22.